Quadriceps myopathy caused by skeletal muscle-specific ablation of β_{cyto}-actin

Kurt W. Prins[1], Jarrod A. Call[2], Dawn A. Lowe[2] and James M. Ervasti[1,*]

[1]Department of Biochemistry, Molecular Biology, and Biophysics, University of Minnesota, Minneapolis, MN 55455, USA
[2]Department of Physical Medicine and Rehabilitation, University of Minnesota, Minneapolis, MN 55455, USA
*Author for correspondence (jervasti@umn.edu)

Accepted 8 November 2010
Journal of Cell Science 124, 951-957

doi:10.1242/jcs.079848

Summary

Quadriceps myopathy (QM) is a rare form of muscle disease characterized by pathological changes predominately localized to the *quadriceps*. Although numerous inheritance patterns have been implicated in QM, several QM patients harbor deletions in dystrophin. Two defined deletions predicted loss of functional spectrin-like repeats 17 and 18. Spectrin-like repeat 17 participates in actin-filament binding, and thus we hypothesized that disruption of a dystrophin–cytoplasmic actin interaction might be one of the mechanisms underlying QM. To test this hypothesis, we generated mice deficient for β_{cyto}-actin in skeletal muscles (*Actb*-msKO). *Actb*-msKO mice presented with a progressive increase in the proportion of centrally nucleated fibers in the *quadriceps*, an approximately 50% decrease in dystrophin protein expression without alteration in transcript levels, deficits in repeated maximal treadmill tests, and heightened sensitivity to eccentric contractions. Collectively, these results suggest that perturbing a dystrophin–β_{cyto}-actin linkage decreases dystrophin stability, which results in a QM, and implicates β_{cyto}-actin as a possible candidate gene in QM pathology.

Key words: Actin, Dystrophin, Myopathy, Skeletal muscle

Introduction

Quadriceps myopathy (QM) is a rare muscle disease predominately affecting the *quadriceps* muscles with clinical symptoms arising in adulthood (Sunohara et al., 1990). There is considerable heterogeneity in QM because etiologies can range from a form of limb-girdle muscular dystrophy (Swash and Heathfield, 1983) to polymyositis (Mohr and Knowlson, 1977; Turner and Heathfield, 1961). Genetic variants of QM are suspected to arise from autosomal dominant (Charniot et al., 2006; Espir and Matthews, 1973), autosomal recessive (Jarry et al., 2007; Mahjneh et al., 2003), and X-linked recessive (Kumari et al., 2000; Wada et al., 1990) inheritance patterns, indicating that several gene products probably play a role in QM pathology. However, multiple reports of alterations in the dystrophin gene, the gene mutated in males afflicted with Duchenne muscular dystrophy (Hoffman et al., 1987), resulted in a QM diagnosis (Beggs et al., 1991; Kumari et al., 2000; Sunohara et al., 1990; Wada et al., 1990).

Molecular characterization of the dystrophin gene in a subset of QM patients predicted deletion of exons 45–48 in one patient (Wada et al., 1990) and deletion of exons 45–47 in three additional patients (Beggs et al., 1991; Kumari et al., 2000). These deletions result in a truncated dystrophin that lacks fully functional spectrin-like repeats 17 and 18. Previous studies indicated that spectrin-like repeat 17 is localized to the second actin binding domain of dystrophin (Amann et al., 1999) and is also important for anchoring neuronal nitric oxide synthase (nNOS) to the sarcolemma (Lai et al., 2009). Moreover, both spectrin-like repeat 17 and 18 can bind anionic phospholipids (Legardinier et al., 2009). Thus, loss of spectrin-like repeats 17 and 18 might compromise interactions between dystrophin and actin filaments, nNOS, anionic phospholipids, or some combination of all three, and possibly explain the underlying defect in this particular subset of QM patients.

Previous studies in mouse models have investigated the function of known binding partners for spectrin-like repeat 17 of dystrophin, but did not observe a QM phenotype. First, nNOS-deficient mice exhibited decreased muscle mass in males (Percival et al., 2008) and increased fatigue following exercise (Kobayashi et al., 2008), but no evidence of muscle cell death, and regeneration was observed (Kobayashi et al., 2008). In regard to the importance of a dystrophin–actin interaction, we showed that dystrophin mechanically linked costameric γ_{cyto}-actin to the sarcolemma (Rybakova et al., 2000). However, skeletal muscle-specific ablation of γ_{cyto}-actin did not result in a QM; instead a myopathy unrelated to dystrophin misregulation was observed (Sonnemann et al., 2006). Collectively, these results indicate that gene deletion of known binding partners of spectrin-like repeat 17 does not result in a QM, which suggests other proteins might also interact with spectrin-like repeat 17 and could potentially be perturbed in this particular subset of QM.

The actin-filament binding activity of spectrin-like repeat 17 (Amann et al., 1999) combined with the fact that dystrophin binds filamentous actin composed of different actin isoforms with similar affinities (Renley et al., 1998) led us to hypothesize that spectrin-like repeat 17 might also interact with β_{cyto}-actin. Although we did not detect β_{cyto}-actin on peeled sarcolemma (Rybakova et al., 2000), another study showed sarcolemmal localization of β_{cyto}-actin on an in situ skeletal muscle preparation (Lubit and Schwartz, 1980). Differences in antibody sources, tissue preparation, and the documented difficulty imaging cytoplasmic actins (Dugina et al., 2009) might explain these seemingly contradictory results. Nonetheless, the results from Lubit et al. indicate dystrophin and β_{cyto}-actin might localize to the same subcellular space in skeletal muscle. Therefore, it is possible that a link between β_{cyto}-actin and dystrophin could be perturbed by the loss of spectrin-like repeat 17.

To investigate the importance of a dystrophin–β_{cyto}-actin interaction in QM pathogenesis, we generated mice that lacked β_{cyto}-actin in skeletal muscle (*Actb*-msKO) by breeding mice that harbored the conditional *Actb* allele to mice expressing Cre recombinase under control of the human α-skeletal actin promoter (Miniou et al., 1999). First, we confirmed β_{cyto}-actin immunostaining at the sarcolemma in control skeletal muscle, which was absent in *Actb*-msKO skeletal muscle. β_{cyto}-actin-deficient skeletal muscle showed a progressive increase in the amount of centrally nucleated fibers, primarily in the *quadriceps*, which was consistent with a QM phenotype. Moreover, ablation of β_{cyto}-actin resulted in a 50% reduction in dystrophin protein levels with no difference in dystrophin transcript levels. Although *Actb*-msKO mice presented with a 50% decrease in dystrophin protein, there was no alteration in cage behavior or reduction in muscle force production. However, significant reductions in performance were recorded when *Actb*-msKO mice were challenged with repeated treadmill tests or eccentric contraction protocols. Collectively, these results suggest loss of a β_{cyto}-actin-dystrophin link results in QM due to decreased dystrophin stability. Finally, our results might provide an explanation for disease associated with disruption of spectrin-like repeats 17 and 18 of dystrophin.

Results

To determine whether disruption of a dystrophin–β_{cyto}-actin interaction results in a QM phenotype, we first generated mice that conditionally lacked β_{cyto}-actin in skeletal muscle. Subsequently, protein levels of actin isoforms were assessed by quantitative western blot analysis of actin-rich eluates from skeletal muscle. *Actb*-msKOs actin extracts showed a 59% reduction in the levels of β_{cyto}-actin, with no detectable compensatory upregulation of γ_{cyto}-, α_{sm}-, or γ_{sm}-actin (Fig. 1,A,B). To determine what cell type was responsible for the remaining β_{cyto}-actin signal observed in *Actb*-msKO skeletal muscle, we subjected control and *Actb*-msKO skeletal muscle sections to immunofluorescence microscopy. Both control mice and *Actb*-msKO sections showed strong β_{cyto}-actin immunoreactivity localizing to endomyosial capillaries (Fig. 1C arrowheads), while a weaker subsarcolemmal staining was observed in control but not *Actb*-msKO (Fig. 1C). Thus, the β_{cyto}-actin present in capillary endothelial cells likely represents the observed β_{cyto}-actin protein detected in *Actb*-msKO skeletal muscle extracts.

We next performed a histological analysis to determine whether *Actb*-msKO mice showed evidence of muscle pathology. At 1 month of age, *Actb*-msKO mice showed no significant pathology in the *tibialis anterior*, *triceps* or *quadriceps* muscles. However as *Actb*-msKO mice aged, significant increases in the proportion of centrally nucleated fibers (CNF) in the *tibialis anterior* (Fig. 2A,B), *triceps* (Fig. 2C,D) and the *quadriceps* (Fig. 2E,F) were recorded. The *quadriceps* was the most affected muscle, with the percentage of CNF progressively increasing to over 13% at 12 months of age. The percentage of CNF in the *triceps* and *tibialis anterior* at 12 months of age were 2.4% and 1.6%, respectively. Further analysis of the pathology in *Actb*-msKO skeletal muscle revealed that the centrally nucleated fibers were confined to fast twitch muscles (supplementary material Fig. S1). Collectively, these results indicate *Actb*-msKO mice possess histopathology consistent with a QM.

Dystrophin protein levels and localization were examined to determine whether the QM in *Actb*-msKO mice was related to dystrophin misregulation. First, we subjected control *quadriceps* cryosections to immunofluorescence microscopy and observed β_{cyto}-actin staining that colocalized with dystrophin at the sarcolemma (Fig. 3A,B). Ablation of β_{cyto}-actin resulted in reductions in dystrophin protein of 44% at 3 months of age and 48% at 12 months (Fig. 3C,D). Decreased dystrophin levels were also associated with a 15% reduction in β-dytroglycan levels at 3 months of age and a 21% reduction at 12 months of age, a 28% reduction in α-sarcoglycan at 3 and 12 months of age, and an increase in utrophin expression of 6% at 3 months of age and a 13% at 12 months of age (Fig. 3C,D). Dystrophin transcript levels did not differ between control and *Actb*-msKO skeletal muscle (Fig. 3E,F), suggesting that a β_{cyto}-actin dystrophin linkage stabilizes dystrophin protein in vivo. Finally, we examined how ablation of β_{cyto}-actin affected dystrophin localization. Although properly localized to the sarcolemma, we observed weaker dystrophin immunofluorescence intensity in *Actb*-msKO skeletal muscle (Fig. 3G), which was consistent with the reduction in total dystrophin protein levels. Finally, we examined costameric organization in *Actb*-msKO mice. Longitudinal sections from *Actb*-msKO *quadriceps* showed that dystrophin was properly localized to costameres with no disruption of costameric organization (Fig.

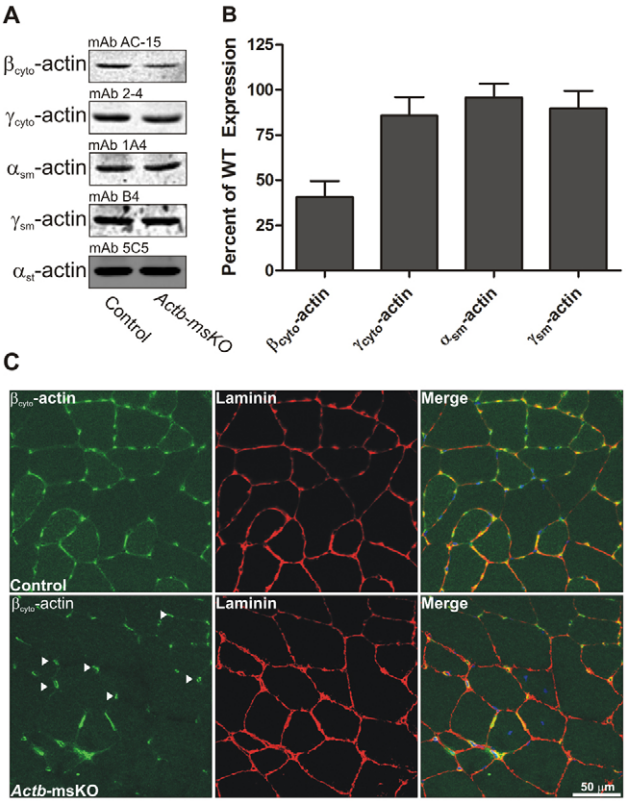

Fig. 1. Skeletal muscle-specific ablation of β_{cyto}-actin. (**A**) Representative western blots of actin isoform expression from actin-rich eluates of skeletal muscle from control and *Actb*-msKO mice. (**B**) Quantification of actin isoform expression from *quadriceps* extracts from three control (WT) and three *Actb*-msKO mice at 3 months of age. α_{st}-actin served as a loading control. *Actb*-msKO skeletal muscle showed a 59% decrease in β_{cyto}-actin expression. Error bars represent s.e.m. (**C**) Cryosections of 10 μm from control and *Actb*-msKO *quadriceps* were stained with DAPI (blue), β_{cyto}-actin (green) and laminin (red). Control skeletal muscle showed sarcolemmal staining, which was absent in *Actb*-msKO skeletal muscle. Endomyosial capillaries (arrowheads) showed strong β_{cyto}-actin immunoreactivity, probably explaining the remaining β_{cyto}-actin signal in actin-rich elutes of *Actb*-msKO muscle. Scale bar: 50 μm.

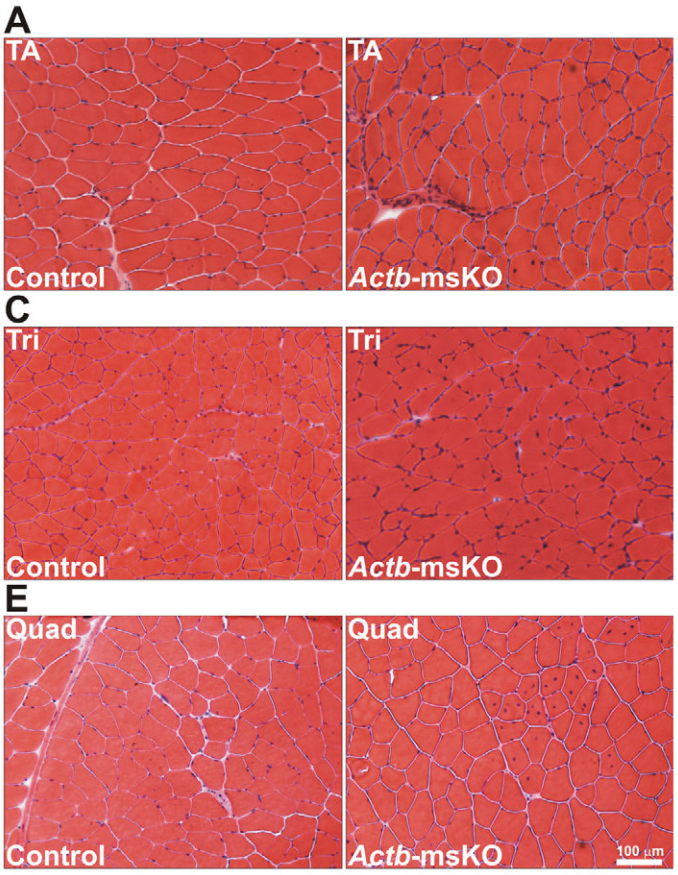

Fig. 2. Quadriceps myopathy in *Actb*-msKO mice.
(**A**–**F**) Representative 10 μm sections stained with hematoxylin and eosin, and respective quantification of the proportion of centrally nucleated fibers from control and *Actb*-msKO *tibialis anterior* (A,B), *triceps* (C,D) and *quadriceps* (E,F) muscles at 1, 3, 6 and 12 months of age (n=3 mice per genotype per timepoint). *$P \leq 0.05$. Error bars represent s.e.m. Scale bar: 100 μm.

3H). In summary, these data suggest that β_{cyto}-actin localizes to the sarcolemma, where it functions to stabilize dystrophin.

Next, we analyzed cage activity and skeletal muscle function in *Actb*-msKO mice. To our surprise, deletion of β_{cyto}-actin did not affect the total distance traveled (Fig. 4A), number of jumps (Fig. 4B), or vertical counts (Fig. 4C) in a 24-hour period. Moreover, *Actb*-msKO showed equivalent in vivo pulling forces (Fig. 4D) and no differences in either twitch or specific force at 3 and 12 months of age (Fig. 4E,F). Collectively, these data indicate that ablation of β_{cyto}-actin mice did not alter cage behavior or result in reduced contractile function.

Finally, we analyzed how ablation of β_{cyto}-actin affected more strenuous tests of muscle performance by subjecting *Actb*-msKO mice to repeated treadmill tests and eccentric contraction protocols. During the first maximal treadmill test, control and *Actb*-msKO mice showed equivalent times to exhaustion (Fig. 5A). However, when the treadmill test was repeated 48 hours later, *Actb*-msKO mice performed significantly worse with an 18% reduction in running time (Fig. 5A). The decreased running time in *Actb*-msKO mice was not associated with altered nNOS localization (supplementary material Fig. S2) or an increase in muscle membrane permeability (Fig. 5B) probably due to preserved interactions between dystrophin and γ_{cyto}-actin (Rybakova et al., 2000), microtubules (Prins et al., 2009), and intermediate filaments (Bhosle et al., 2006; Stone et al., 2005). Subsequently, we assayed damage contractile deficits caused by eccentric contractions both both ex vivo and in vivo. At both 3 and 12 months of age, isolated *extensor digitorum longus* muscles from *Actb*-msKO mice showed a significant increase in force drop following five consecutive eccentric contractions (Fig. 5C). The in vivo eccentric contraction protocol resulted in reduced contractile performance in both controls and *Actb*-msKOs (Fig. 5D); however, two-way ANOVA indicated that a significant column factor exists when comparing control and *Actb*-msKO mice (Fig. 5D). By calculating the contraction number at which torque loss was within 2% of the total loss, we observed that *Actb*-msKOs reached their final torque significantly faster than controls (Fig. 5E). These results indicate that eccentric-contraction-induced damage in vivo occurs more readily when β_{cyto}-actin is deleted. In summary, these data demonstrate that loss of β_{cyto}-actin renders skeletal muscle more susceptible to damage during maximal treadmill tests and eccentric contractions.

Discussion

Although skeletal muscle-specific ablation of β_{cyto}-actin led to a QM phenotype, *Actb*-msKO mice lacked the muscle weakness and muscle atrophy phenotypes observed in QM patients expressing dystrophin that lacked spectrin-like repeats 17 and 18. Because spectrin-like repeats 17 and 18 interact with nNOS and lipids, it is likely that patients expressing a dystrophin without spectrin-like repeats 17 and 18 have a compound molecular phenotype. In fact, reduced muscle size in male mice lacking nNOS (Percival et al., 2008) combined with our results more accurately recapitulates this particular QM. However, it is important to note that mouse models do not always phenocopy all aspects of human disease. For instance, the dystrophin-deficient *mdx* mouse experiences a disease much less severe than that experienced by Duchenne patients (Banks and Chamberlain, 2008). Nonetheless, the QM phenotype of *Actb*-msKO mice suggests that disruption of a dystrophin–β_{cyto}-actin

interaction could be one of the molecular deficits caused by deletion of spectrin-like repeats 17 and 18 of dystrophin.

The more severe phenotype observed in the *quadriceps* muscle as compared to the *triceps* and *tibialis anterior* muscles is probably due to the different physiological loads each muscle bears and not to different cellular phenotypes in different skeletal muscles. Consistent with this hypothesis, we observed a 42% decrease in dystrophin protein levels in the *triceps* extracts (supplementary material Fig. S3), providing evidence to support the idea that a similar cellular phenotype is present in all skeletal muscles. Moreover, skeletal muscles that support minimal amounts of body weight in vivo, the *extensor digitorium longus* and the *diaphragm*, showed minimal evidence of muscle cell necrosis. The diaphragm did not exhibit a significant increase in the proportion of centrally nucleated fibers; however, the *extensor digitorium longus* did show a small (1.9%) but significant increase in histopathology (supplementary material Fig. S4). Collectively, these results suggest that all skeletal muscles possess the same cellular phenotype; however, different physiological demands result in different amounts of histopathological changes, with the muscles bearing more body weight being most affected.

We hypothesize that disruption of a dystrophin–β_{cyto}-actin interaction reduces dystrophin stability in *Actb*-msKO mice and probably leads to the muscle phenotypes observed. Consistent with this hypothesis, a transgenic mouse expressing approximately 40% of normal levels of dystrophin exhibited levels of centrally nucleated fibers in the *quadriceps* (Phelps et al., 1995) that were comparable to those observed in our studies. Interestingly, truncated dystrophin constructs that contain only one actin binding domain, which probably reduces binding to β_{cyto}-actin, can rescue most phenotypes of the dystrophin-deficient *mdx* mouse (Friedrich et al., 2004; Gregorevic et al., 2004; Gregorevic et al., 2006; Harper et al., 2002). However, in these studies dystrophin constructs were expressed at supraphysiological levels, and thus were probably able to overcome the reduced protein stability due to decreased interactions with β_{cyto}-actin. Another transgenic line of mice expressing subphysiological levels of a dystrophin construct lacking the second actin binding domain displayed evidence of muscle cell death (Wells et al., 1995). Moreover, the truncated dystrophin did not associate with membrane preparations as effectively as full-length dystrophin (Wells et al., 1995), providing more evidence to

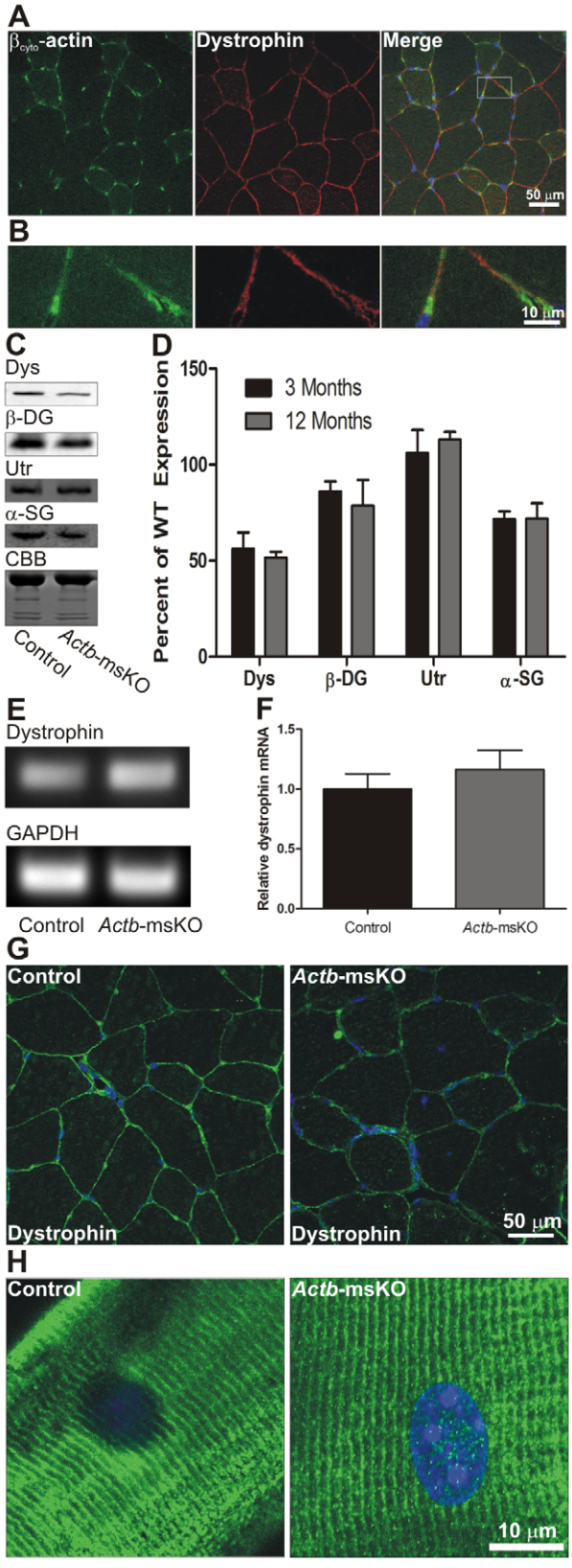

Fig. 3. β_{cyto}-actin colocalizes with dystrophin and is necessary for dystrophin stability. (**A**) Cryosections of 10 μm from control *quadriceps* were stained with β_{cyto}-actin (green) and dystrophin (red). (**B**) Higher magnification image of box from A. Dystrophin and β_{cyto}-actin colocalize at the sarcolemma. (**C**) Representative western blots of dystrophin (Dys), β-dystroglycan (DG), utrophin(Utr) and α-sarcoglycan (SG) from SDS-extracted skeletal muscle. Post-transfer Coomassie Brilliant Blue (CBB)-stained gel shows equivalent loading. The most prominent band represents myosin heavy chain. (**D**) Quantification of dystrophin, β-dystroglycan, utrophin and α-sarcoglycan expression from skeletal muscle of 3- and 12-month-old *Actb*-msKO mice. Dystrophin expression was decreased approximately 50%, β-dystroglycan expression was decreased approximately 15–20%, utrophin levels were increased 6–13%, and α-sarcoglycan expression was decreased approximately 28% compared with control skeletal muscle. Error bars represent s.e.m. (**E**) Ethidium bromide-stained agarose gel showing quantitative RT-PCR products of dystrophin and GAPDH. (**F**) Quantification of dystrophin transcript normalized to GAPDH. Ablation of β_{cyto}-actin did not alter dystrophin transcript levels. (**G**) Cryosections of 10 μm from control and *Actb*-msKO *quadriceps* were stained with dystrophin (green) and DAPI (blue). Ablation of β_{cyto}-actin led to decreased dystrophin staining at the sarcolemma. (**H**) Longitudinal sections of 20 μm from control and *Actb*-msKO *quadriceps* were stained with dystrophin (green) and DAPI (blue). Costamere organization is preserved in *Actb*-msKO skeletal muscle.

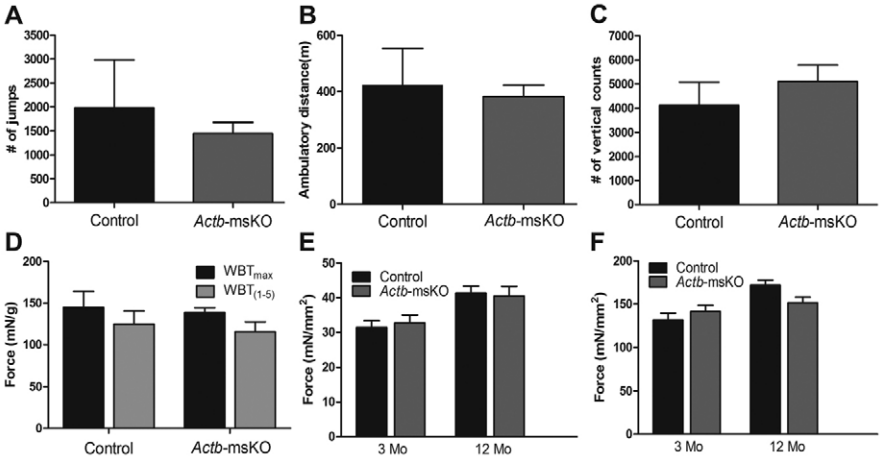

Fig. 4. Ablation of β_{cyto}-actin does not alter cage behavior or force-generating capacity. (**A**–**C**) Quantification of 24-hour cage behavior in control (n=6) and *Actb*-msKO (n=7) mice indicated there was no significant decrease in the number of jumps (A), ambulatory distance (B), or the number of vertical counts (C) in *Actb*-msKO mice at 3–4 months of age. (**D**–**F**) Whole body tension (D), twitch force (E) and specific force (F) were not altered by ablation of β_{cyto}-actin. Error bars represent s.e.m.

suggest that an interaction between dystrophin and β_{cyto}-actin increases dystrophin stability.

Finally, the QM phenotype of *Actb*-msKO mice makes the *ACTB* gene a possible target to investigate in patients with an undefined QM. However, a QM would probably only be one of many symptoms associated with expression of a mutant β_{cyto}-actin due to its ubiquitous expression. In fact, two mutations in the *ACTB* gene were associated with numerous physiological deficits ranging from immunodeficiency (Nunoi et al., 1999) to dystonia and hearing loss (Procaccio et al., 2006). Both the complexity of symptoms as well as premature death might have precluded detection of a QM in these patients. Nonetheless, our results demonstrate that ablation of β_{cyto}-actin results in a QM and, therefore, these data could help define future cases of QM-associated syndromes.

Materials and Methods

Mice

Mice harboring the conditional *Actb* allele were described previously (Perrin et al., 2010) and subsequently backcrossed a minimum of five generations to the C57BL/6 background. These mice were crossed to mice expressing cre recombinase under control of the human α_{sk}-actin promoter (HSA-Cre mice were provided by Judith Melki, INSERM, Evry, France) to generate mice that were homozygous for the floxed *Actb* allele and hemizygous for HSA-Cre. Homozygous 'floxed' mice not harboring the cre transgene served as controls. Both males and females exhibited similar phenotypes and therefore the results from both genders were pooled. Genotypes of the *Actb* locus and presence of the cre transgene were determined using PCR as described (Sonnemann et al., 2006; Perrin et al., 2010). All animals were housed and treated in accordance with the standards set forth by the University of Minnesota Institutional Animal Care and Use Committee.

Antibodies

Monoclonal antibody to γ_{cyto}-actin was described previously (Hanft et al., 2006). Monoclonal antibodies to β_{cyto}-actin (AC-15), α_{sm}-actin (1A4), α_{st}-actin (5C5), slow myosin heavy chain (NOQ7.5.4D), fast myosin heavy chain (MY-32) and a polyclonal antibody to laminin (catalogue number L9393) were purchased from Sigma. The monoclonal γ_{sm}-actin antibody (B4) was provided as a kind gift from James Lessard (Cincinnati Children's Medical Center, Cincinnati, OH). Monoclonal antibodies to dystrophin (Dys2) and α-sarcoglycan (a-SARC) were purchased from Novacastra. The monoclonal β-dystroglycan antibody (43DAG-1) was purchased from Vector Laboratories. The polyclonal nNOS antibody (sc-648) and the monoclonal utrophin antibody (8A4) were purchased from Santa Cruz Biotechnology. Polyclonal dystrophin antibody (Rb2) was described previously (Rybakova et al., 1996). Infrared dye-conjugated anti-mouse and anti-rabbit antibodies were purchased from LICOR Biosciences. The monoclonal FITC-conjugated β_{cyto}-actin antibody was purchased from Abcam. Alexa-Fluor-488- or Alexa-Fluor-568-conjugated anti-rabbit antibodies were purchased from Molecular Probes.

Muscle extracts

Muscle was harvested from anesthetized mice immediately following cervical dislocation, and snap frozen in liquid N_2. Samples of 100 mg of *quadriceps* or *triceps* muscle were pulverized in a liquid N_2 cooled mortar and pestle and subjected to SDS extraction as described (Hanft et al., 2006). Protein concentration was

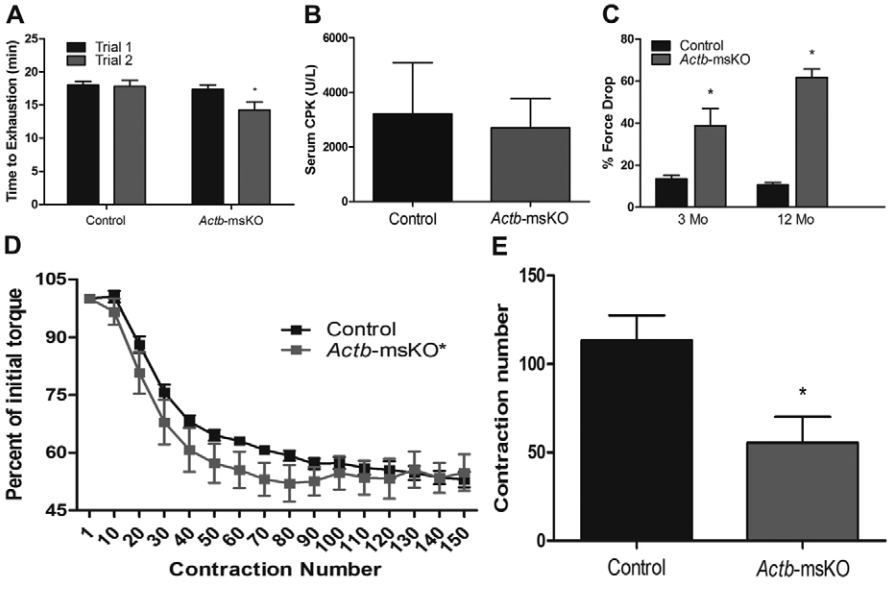

Fig. 5. *Actb*-msKO skeletal muscle shows increased susceptibility to stressful stimuli. (**A**) Repeated maximal treadmill tests show a significant reduction in running time on the second trial in *Actb*-msKO mice. (**B**) Quantification of serum CK activity following treadmill test. *Actb*-msKO did not exhibit elevated sarcolemmal permeability. (**C**) Percentage force drop following five eccentric contractions on isolated *extensor digitorum longus* muscles. At 3 and 12 months of age, *Actb*-msKO muscle was significantly more susceptible to eccentric-contraction-induced force loss. (**D**) Quantification of force production from an in vivo eccentric contraction protocol testing the anterior leg compartment of control and *Actb*-msKO mice indicates a statistically significant column factor exists as determined by Two-way ANOVA. (**E**) Contraction number when force drop percentage was within 2% of final force drop percentage. *Actb*-msKO mice reached their final force drop percentage significantly faster than control mice. *$P \leq 0.05$ compared with control values, as determined by t-test.

determined using the Bio-Rad DC Protein Assay. Actin preparations from skeletal muscle were collected by subjecting muscle to a low-salt extraction and DNase-1 amplification protocol as described (Hanft et al., 2006).

Immunofluorescence analysis

Quadriceps and *triceps* muscles were dissected, coated in optimum cutting temperature (OCT) medium from TissueTek, and then frozen in melting isopentane. Transverse sections of 10 µm were cut on a Leica CM3050 cryostat, air dried, and then fixed in 4% paraformaldehyde for 10 minutes. Sections were washed with PBS (150 mM NaCl, 8 mM NaH_2PO_4, 42 mM Na_2HPO_4), blocked in 5% goat serum for 30 minutes, and incubated with primary antibodies overnight at 4°C. Primary antibody dilutions were: pAb anti-laminin (1:1000), pAb Rb2 (1:1000), pAb anti-nNOS (1:50), mAb anti-FMHC (1:100) and mAb anti SMHC (1:100). Sections were then washed and blocked with 5% goat serum for 10 minutes three times and then incubated with Alexa-Fluor-488- or Alexa-Fluor-568-conjugated secondary antibodies (1:1000 dilution) for 30 minutes at 37°C. Then, sections were washed with PBS and coverslips were applied with a drop of Anti-Fade Reagent (Molecular Probes). Confocal images were collected on a Bio-Rad MRC 1000 scan head mounted on an upright Nikon Optishot microscope at the University of Minnesota Biomedical Image Processing Laboratory. Images were equivalently processed using Adobe Photoshop 6.0.

When the monoclonal FITC-conjugated β_{cyto}-actin was used, sections were fixed in 4% paraformaldehyde for 10 minutes, post-fixed in 100% methanol at –20°C for 10 minutes and subjected to immunofluorescence staining as described in previous paragraph. The dilution of the monoclonal FITC-conjugated β_{cyto}-actin was 1:50 and the antibody was added during the secondary antibody incubation step. When using the nNOS antibody, sections were fixed in 100% methanol at –20°C, and subjected to immunofluorescence as described in previous paragraph.

For costameric imaging, *quadriceps* were frozen in melting isopentane and 20 µm sections were collected and subjected to immunofluorescence staining as described above with one exception: the Rb2 antibody was used at a 1:500 dilution.

Histological assessment

Quadriceps, *tibialis anterior*, *extensor digitorium longus, diaphragm* and *triceps* muscles were dissected, coated in OCT, and then frozen in melting isopentane. Transverse sections of 10 µm were cut on a Leica CM3050 cryostat and stained with hematoxylin and eosin-phloxine as described. Montage images of the entire sections were collected using ImagePro Software. The montages were then analyzed in ImagePro and every fiber in the section was scored to determine the proportion of centrally nucleated fibers in 1-, 3- and 12-month-old mice (n=3 for each genotype at each timepoint). Pathology in the *extensor digitorium longus* and the *diaphragm* was examined in 10- to 12-month-old mice.

Measurement of sarcolemma permeability

Membrane permeability was determined by quantifying serum creatine kinase levels on Vitros CK DT slides (Ortho-Clinical Diagnostics) using a Kodak Ektachem DT60 analyzer.

Western blot analysis and quantification

Western blot analysis and quantification of skeletal muscle extracts (n=3 for control and *Actb*-msKO at both 3 and 12 months of age) and actin-rich elutes (n=3 for control and *Actb*-msKO mice at 3 months of age) was performed as described (Prins et al., 2008). Briefly, 25 µg of skeletal muscle extract or 20 µl of actin-rich elutes were subjected to SDS-PAGE and transferred to nitrocellulose membranes, which were washed and blocked in a 5% milk solution in PBS for 1 hour. Then, the membranes were incubated overnight with primary antibody at room temperature. Primary antibodies and dilutions employed were: mAb Dys2 (1:50), mAb 43DAG-1 (1:50), mAb a-SARC (1:50), mAb 8A4 (1:50), mAb 2-4 (1:500), mAb AC-15 (1:100), mAb B4 (1:100), mAb 1A4 (1:100) and mAb 5C5 (1:1000). Membranes were washed twice for 10 minutes in 5% milk solution at room temperature, incubated with IR-dye-conjugated secondary antibody (1:10,000 dilution) for 30 minutes at room temperature, and then the membranes were washed in a 0.5% Tween solution in PBS twice for 10 minutes. Western blots were imaged and quantified with an Odyssey Infrared Imaging System. The Coomassie Blue-stained post-transfer gel was analyzed densitometrically using UVP software and served as the loading control.

Quantitative real-time PCR

Total RNA was isolated from skeletal muscle from four control and four *Actb*-msKO mice using TRIzol reagent (Invitrogen) according to the manufacturer's instructions. RNA was treated with RNase-free DNase (Ambion) at room temperature for 15 minutes. cDNA was generated using the iScript cDNA synthesis kit (Bio-Rad). For RT-PCR, cDNA was amplified using the SYBR GreenER qPCR ReadyMix (Invitrogen) on the Bio-Rad iQ5. Results of quantitative RT-PCR assays were analyzed using analysis software supplied with the Bio-Rad iQ5 system to determine dystrophin transcript levels (dystrophin forward 5′-AATGGCCTGCCCTGGGGGAT-3′, dystrophin reverse 5′-TCTGGTGTAGACCTGGCGGC-3′) normalized to GAPDH transcript levels (GAPDH forward 5′-GACCCCTCCATTGACCTCA-ACTACATG-3′, GAPDH reverse 5′-CTCCTGGAAGATGGTGATGGG-3′).

Whole body tension

Whole body tension (WBT) was performed as described (Sonnemann et al., 2006). Briefly, 3-month-old control and *Actb*-msKO mice (n=4 for each genotype) were tied with silk suture to a fixed range force transducer (BioPac Systems) to record the force evoked by a light tail pinch. Data were analyzed by comparing WBT_1 (the maximal force produced by each mouse) and $WBT_{1–5}$ (the average of the top five force-producing pulls), with both being normalized to body weight.

Activity measurements

Mice of 3–4 months of age (n=6 control, n=7 *Actb*-msKO) were monitored for 24-hour cage activities using activity chambers (Med Associates) as described (Landisch et al., 2008). In brief, mice were exposed to a 24-hour acclimation period in a mock chamber, which was identical to the activity-monitoring cage except that it lacked the infrared arrays. The activity chambers contain three infrared arrays in the x-, y-, and z-axes, with two sets of beams in the x-direction, one being elevated above the other. Ambulation was measured by arrays located in the x- and y-axes, and vertical movement (i.e., jumping and hindlimb rearing) was measured by the second elevated x-array. Infrared sensors in the chamber registered an activity count each time one of the beams was disrupted, such that movement was simultaneously measured in all three axes. All data were acquired using Activity Monitor software, version 5 (Med Associates).

Ex vivo extensor *digitorium longus* contractile properties

Mice of 3 months and 11–12 months were anesthetized and the *extensor digitorum longus* muscle was removed (n=4 mice per genotype per timepoint). The proximal tendon was attached to 4–0 suture silk to a dualmode muscle lever system (model 300B-LR Aurora Scientific, Aurora, ON, Canada). Muscles were equilibrated for 10 minutes in a bath assembly containing Krebs–Ringer–bicarbonate buffer (119 mM NaCl, 5.0 KCl mM, 1.0 $MgSO_4$ mM, 12.25 $NaHCO_3$ mM, 1.0 $CaCl_2$ mM, 1.0 mM KH_2PO_4, 10.0 mM glucose, 0.17 mM leucine, 0.10 mM isoleucine, 0.20 mM valine plus 10 mg/ml gentamicin sulfate and 0.10 U/ml insulin) at 25°C while being constantly oxygenated with 95% O_2 and 5% CO_2 gas. Then, the resting tension was set to 0.4 g and twitch force was determined by stimulating the muscle with a 0.5 millisecond pulse at 150 V (Grass stimulator, Grass Telefactor). Thirty seconds later, the muscle was stimulated to twitch again and the greater of two contractions was recorded. Tetanic contractions were elicited by stimulating the muscle with 150 V for 200 milliseconds at 180 Hz. The greater of two contractions separated by 2 minutes of recovery time was recorded. To determine damage caused by eccentric contractions muscles were subjected to five lengthening contractions at 3-minute intervals. Each eccentric contraction consisted of a maximal tetanic stimulation for 200 milliseconds accompanied by a stretch of 1.0 L_0/second (where L_0 is the optimal muscle length for maximal force) to give a total stretch of 0.2 L_0. Force drop was calculated as $(ECC_1–ECC_5)/ECC_1$, where ECC_1 is the peak force generated on the first eccentric contraction and ECC_5 is the force generated on the fifth eccentric contraction.

In vivo eccentric contraction

In vivo eccentric contraction was carried out as previously described (Baltgalvis et al., 2009). First, mice were given a mixture of fentanyl citrate (10 mg/kg body weight), droperidol (0.2 mg/kg weight) and diazepam (5 mg/kg weight), and then the hair on the left hindlimb was shaved and removed with depilatory cream. The left foot of the mouse was taped to a metal foot plate, which was connected to the shaft of the servomotor (model 300B-LR, Aurora Scientific) with the left knee stabilized, ensuring the tibia was perpendicular to the foot. Two sterilized platinum subdermal needle electrodes (model E2-12, Grass Technologies) were inserted through the skin 1–2 mm on either side of the left common peroneal nerve. The servomotor passively dorsiflexed the foot 20° over a duration of 3 seconds, and the nerve was stimulated while the foot was plantar flexed 40° at a velocity of 2000°/second to generate eccentric contractions. After the stimulation, the foot was passively dorsiflexed 20° to its original resting position over a 3-second period. One contraction was performed every 12 seconds for a total of 150 eccentric contractions.

Treadmill exhaustion test

Maximal exercise performance studies were performed on a Columbus Instruments treadmill with an uphill grade of 15°. An acclimation period of running at a speed of 10 m/minute for 5 minutes twice a week for 2 weeks was implemented prior to maximal testing. To determine maximal exercise performance, mice were run on the treadmill for 5 minutes at a rate of 10 m/minute followed by a 1 m/minute increase in speed every minute until exhaustion. Exhaustion was defined as an inability to stay off a shock bar for at least 5 seconds. Maximal exercise capacity was determined twice, with the trials being separated by 48 hours.

Statistical analysis

All data are presented as mean ± s.e.m. Comparison between groups was performed using a t-test with significance defined as $P \leq 0.05$. When comparing the response of two groups over time, two-way ANOVA was implemented and significance was defined as $P \leq 0.05$.

The authors thank Sarah Greising for assistance in the cage behavior monitoring, Kevin Sonneman for generating mice with a conditional *Actb* allele, and Thomas Cheever and Emily Olson for their helpful discussion. This work was funded by an NIH grant AR049899. K.W.P. is a member of the Medical Scientist Training Program at the University of Minnesota. Deposited in PMC for release after 12 months.

Supplementary material available online at
http://jcs.biologists.org/cgi/content/full/124/6/951/DC1

References

Amann, K. J., Guo, A. W. and Ervasti, J. M. (1999). Utrophin lacks the rod domain actin binding activity of dystrophin. *J. Biol. Chem.* **274,** 35375-35380.

Baltgalvis, K. A., Call, J. A., Nikas, J. B. and Lowe, D. A. (2009). Effects of prednisolone on skeletal muscle contractility in mdx mice. *Muscle Nerve* **40**, 443-454.

Banks, G. B. and Chamberlain, J. S. (2008). The value of mammalian models for duchenne muscular dystrophy in developing therapeutic strategies. *Curr. Top. Dev. Biol.* **84**, 431-453.

Beggs, A. H., Hoffman, E. P., Snyder, J. R., Arahata, K., Specht, L., Shapiro, F., Angelini, C., Sugita, H. and Kunkel, L. M. (1991). Exploring the molecular basis for variability among patients with becker muscular dystrophy: Dystrophin gene and protein studies. *Am. J. Hum. Genet.* **49**, 54-67.

Bhosle, R. C., Michele, D. E., Campbell, K. P., Li, Z. and Robson, R. M. (2006). Interactions of intermediate filament protein synemin with dystrophin and utrophin. *Biochem. Biophys. Res. Commun.* **346**, 768-777.

Charniot, J. C., Desnos, M., Zerhouni, K., Bonnefont-Rousselot, D., Albertini, J. P., Salama, J. Z., Bassez, G., Komajda, M. and Artigou, J. Y. (2006). Severe dilated cardiomyopathy and quadriceps myopathy due to lamin A/C gene mutation: A phenotypic study. *Eur. J. Heart Fail.* **8**, 249-256.

Dugina, V., Zwaenepoel, I., Gabbiani, G., Clement, S. and Chaponnier, C. (2009). Beta and gamma-cytoplasmic actins display distinct distribution and functional diversity. *J. Cell Sci.* **122**, 2980-2988.

Espir, M. L. and Matthews, W. B. (1973). Hereditary quadriceps myopathy. *J. Neurol. Neurosurg. Psychiatr.* **36**, 1041-1045.

Friedrich, O., Both, M., Gillis, J. M., Chamberlain, J. S. and Fink, R. H. (2004). Mini-dystrophin restores L-type calcium currents in skeletal muscle of transgenic mdx mice. *J. Physiol.* **555**, 251-265.

Gregorevic, P., Blankinship, M. J., Allen, J. M., Crawford, R. W., Meuse, L., Miller, D. G., Russell, D. W. and Chamberlain, J. S. (2004). Systemic delivery of genes to striated muscles using adeno-associated viral vectors. *Nat. Med.* **10**, 828-834.

Gregorevic, P., Allen, J. M., Minami, E., Blankinship, M. J., Haraguchi, M., Meuse, L., Finn, E., Adams, M. E., Froehner, S. C., Murry, C. E. et al. (2006). rAAV6-microdystrophin preserves muscle function and extends lifespan in severely dystrophic mice. *Nat. Med.* **12**, 787-789.

Hanft, L. M., Rybakova, I. N., Patel, J. R., Rafael-Fortney, J. A. and Ervasti, J. M. (2006). Cytoplasmic gamma-actin contributes to a compensatory remodeling response in dystrophin-deficient muscle. *Proc. Natl. Acad. Sci. USA* **103**, 5385-5390.

Harper, S. Q., Hauser, M. A., DelloRusso, C., Duan, D., Crawford, R. W., Phelps, S. F., Harper, H. A., Robinson, A. S., Engelhardt, J. F., Brooks, S. V. et al. (2002). Modular flexibility of dystrophin: Implications for gene therapy of duchenne muscular dystrophy. *Nat. Med.* **8**, 253-261.

Hoffman, E. P., Brown, R. H., Jr and Kunkel, L. M. (1987). Dystrophin: The protein product of the duchenne muscular dystrophy locus. *Cell* **51**, 919-928.

Jarry, J., Rioux, M. F., Bolduc, V., Robitaille, Y., Khoury, V., Thiffault, I., Tetreault, M., Loisel, L., Bouchard, J. P. and Brais, B. (2007). A novel autosomal recessive limb-girdle muscular dystrophy with quadriceps atrophy maps to 11p13-p12. *Brain* **130**, 368-380.

Kobayashi, Y. M., Rader, E. P., Crawford, R. W., Iyengar, N. K., Thedens, D. R., Faulkner, J. A., Parikh, S. V., Weiss, R. M., Chamberlain, J. S., Moore, S. A. et al. (2008). Sarcolemma-localized nNOS is required to maintain activity after mild exercise. *Nature* **456**, 511-515.

Kumari, D., Gupta, M. and Goyle, S. (2000). Detection of deletion in the dystrophin gene of a patient with quadriceps myopathy. *Neurol. India* **48**, 68-71.

Lai, Y., Thomas, G. D., Yue, Y., Yang, H. T., Li, D., Long, C., Judge, L., Bostick, B., Chamberlain, J. S., Terjung, R. L. et al. (2009). Dystrophins carrying spectrin-like repeats 16 and 17 anchor nNOS to the sarcolemma and enhance exercise performance in a mouse model of muscular dystrophy. *J. Clin. Invest.* **119**, 624-635.

Landisch, R. M., Kosir, A. M., Nelson, S. A., Baltgalvis, K. A. and Lowe, D. A. (2008). Adaptive and nonadaptive responses to voluntary wheel running by mdx mice. *Muscle Nerve* **38**, 1290-1303.

Legardinier, S., Raguenes-Nicol, C., Tascon, C., Rocher, C., Hardy, S., Hubert, J. F. and Le Rumeur, E. (2009). Mapping of the lipid-binding and stability properties of the central rod domain of human dystrophin. *J. Mol. Biol.* **389**, 546-558.

Lubit, B. W. and Schwartz, J. H. (1980). An antiactin antibody that distinguishes between cytoplasmic and skeletal muscle actins. *J. Cell Biol.* **86**, 891-897.

Mahjneh, I., Somer, H., Paetau, A. and Marconi, G. (2003). Pure quadriceps myopathy in two sisters. *Eur. J. Neurol.* **10**, 453-456.

Miniou, P., Tiziano, D., Frugier, T., Roblot, N., Le Meur, M. and Melki, J. (1999). Gene targeting restricted to mouse striated muscle lineage. *Nucleic Acids Res.* **27,** e27.

Mohr, P. D. and Knowlson, T. G. (1977). Quadriceps myositis: An appraisal of the diagnostic criteria of quadriceps myopathy. *Postgrad. Med. J.* **53**, 757-760.

Nunoi, H., Yamazaki, T., Tsuchiya, H., Kato, S., Malech, H. L., Matsuda, I. and Kanegasaki, S. (1999). A heterozygous mutation of beta-actin associated with neutrophil dysfunction and recurrent infection. *Proc. Natl. Acad. Sci. USA* **96**, 8693-8698.

Percival, J. M., Anderson, K. N., Gregorevic, P., Chamberlain, J. S. and Froehner, S. C. (2008). Functional deficits in nNOSmu-deficient skeletal muscle: Myopathy in nNOS knockout mice. *PLoS One* **3**, e3387.

Perrin, B. J., Sonnemann, K. J. and Ervasti, J. M. (2010). β-actin and γ-actin are each dispensible for auditory hair cell development but required for stereocilia maintenance. *PLoS Genet.* **6**, e1001158.

Phelps, S. F., Hauser, M. A., Cole, N. M., Rafael, J. A., Hinkle, R. T., Faulkner, J. A. and Chamberlain, J. S. (1995). Expression of full-length and truncated dystrophin mini-genes in transgenic mdx mice. *Hum. Mol. Genet.* **4**, 1251-1258.

Prins, K. W., Lowe, D. A. and Ervasti, J. M. (2008). Skeletal muscle-specific ablation of gamma(cyto)-actin does not exacerbate the mdx phenotype. *PLoS One* **3**, e2419.

Prins, K. W., Humston, J. L., Mehta, A., Tate, V., Ralston, E. and Ervasti, J. M. (2009). Dystrophin is a microtubule-associated protein. *J. Cell Biol.* **186**, 363-369.

Procaccio, V., Salazar, G., Ono, S., Styers, M. L., Gearing, M., Davila, A., Jimenez, R., Juncos, J., Gutekunst, C. A., Meroni, G. et al. (2006). A mutation of beta -actin that alters depolymerization dynamics is associated with autosomal dominant developmental malformations, deafness, and dystonia. *Am. J. Hum. Genet.* **78**, 947-960.

Renley, B. A., Rybakova, I. N., Amann, K. J. and Ervasti, J. M. (1998). Dystrophin binding to nonmuscle actin. *Cell Motil. Cytoskeleton* **41**, 264-270.

Rybakova, I. N., Amann, K. J. and Ervasti, J. M. (1996). A new model for the interaction of dystrophin with F-actin. *J. Cell Biol.* **135**, 661-672.

Rybakova, I. N., Patel, J. R. and Ervasti, J. M. (2000). The dystrophin complex forms a mechanically strong link between the sarcolemma and costameric actin. *J. Cell Biol.* **150**, 1209-1214.

Sonnemann, K. J., Fitzsimons, D. P., Patel, J. R., Liu, Y., Schneider, M. F., Moss, R. L. and Ervasti, J. M. (2006). Cytoplasmic gamma-actin is not required for skeletal muscle development but its absence leads to a progressive myopathy. *Dev. Cell* **11**, 387-397.

Stone, M. R., O'Neill, A., Catino, D. and Bloch, R. J. (2005). Specific interaction of the actin-binding domain of dystrophin with intermediate filaments containing keratin 19. *Mol. Biol. Cell* **16**, 4280-4293.

Sunohara, N., Arahata, K., Hoffman, E. P., Yamada, H., Nishimiya, J., Arikawa, E., Kaido, M., Nonaka, I. and Sugita, H. (1990). Quadriceps myopathy: Forme fruste of becker muscular dystrophy. *Ann. Neurol.* **28**, 634-639.

Swash, M. and Heathfield, K. W. (1983). Quadriceps myopathy: A variant of the limb-girdle dystrophy syndrome. *J. Neurol. Neurosurg. Psychiatr.* **46**, 355-357.

Turner, J. W. and Heathfield, K. W. (1961). Quadriceps myopathy occurring in middle age. *J. Neurol. Neurosurg. Psychiatr.* **24**, 18-21.

Wada, Y., Itoh, Y., Furukawa, T., Tsukagoshi, H. and Arahata, K. (1990). "Quadriceps myopathy": A clinical variant form of becker muscular dystrophy. *J. Neurol.* **237**, 310-312.

Wells, D. J., Wells, K. E., Asante, E. A., Turner, G., Sunada, Y., Campbell, K. P., Walsh, F. S. and Dickson, G. (1995). Expression of human full-length and minidystrophin in transgenic mdx mice: Implications for gene therapy of duchenne muscular dystrophy. *Hum. Mol. Genet.* **4**, 1245-1250.